Functionally enhanced placenta-derived mesenchymal stem cells inhibit adipogenesis in orbital fibroblasts with Graves' ophthalmopathy

Jae Yeon Kim
CHA University
Sohae Park
CHA University
Hyun-Jung Lee
CHA University
Helen Lew
CHA Bundang Medical Center
Gi Jin Kim (gjkim@cha.ac.kr)
CHA University https://orcid.org/0000-0002-2320-7157

Research

Keywords: Adipogenesis, Graves' ophthalmopathy, Gene modification, Phosphatase of regenerating liver-1, Placenta-derived mesenchymal stem cells

Posted Date: June 25th, 2020

DOI: https://doi.org/10.21203/rs.2.23922/v2

Version of Record: A version of this preprint was published on November 5th, 2020. See the published version at https://doi.org/10.1186/s13287-020-01982-3.

Abstract

Background: Placenta-derived mesenchymal stem cells (PD-MSCs) have unique immunomodulatory properties, and phosphatase of regenerating liver-1 (PRL-1) regulates the self-renewal ability of stem cells and promotes proliferation. Graves' ophthalmopathy (GO) is an autoimmune inflammatory disease of the orbit and is characterized by increased orbital levels of adipose tissue. Because the mechanism of inhibiting adipogenesis in orbital fibroblast (OF) with GO patients remains uncertain, the major objective of the present study is to investigate the mechanisms by which PRL-1-overexpressing PD-MSCs (PD-MSCs^{PRL-1}, PRL-1+) alleviate adipogenesis in OFs derived from GO patients.

Methods: Primary OFs were isolated from orbital adipose tissue specimens from GO patients. After maturation as adipogenic differentiation, normal and GO-derived OFs were cocultured with naïve PD-MSCs and PD-MSCs^{PRL-1}. Western blotting was conducted to evaluate the molecular mechanisms associated with adipogenesis inhibition in GO.

Results: The characteristics of PD-MSCs^{PRL-1} were similar to those of naïve cells. OFs from GO patients underwent stimulated adipocyte differentiation and had significantly decreased lipid accumulation after coculture with PD-MSCs^{PRL-1} compared with naïve cell coculture. The mRNA and protein expression of adipogenic markers was decreased in PD-MSCs^{PRL-1}. The protein expression of phosphorylated PI3K/AKT/mTOR in OFs from GO patients was downregulated by coculture with PD-MSCs^{PRL-1}, which secreted IGFBPs. Interestingly, IGFBP2, -4, and -7 expression in PD-MSCs^{PRL-1}, which was mediated by integrin alpha 4 (ITGA4) and integrin beta 7 (ITGB7), was higher than that in naïve cells and upregulated phosphorylated focal adhesion kinase (pFAK) downstream factors.

Conclusion: In summary, PD-MSC^{PRL-1}-secreted IGFBPs inhibit adipogenesis in OFs from GO patients by upregulating FAK and blocking IGF, providing a novel therapeutic strategy using functionally enhanced MSCs to treat degenerative diseases.

Background

Graves' ophthalmopathy (GO) is a thyroid-associated autoimmune disease of the eye that is potentially sight-threatening. The main symptoms of GO are proptosis-associated impairment of eye motility, lid retraction, de novo adipogenesis, and soft tissue inflammation. In particular, inflammatory reactions of orbital fibroblasts (OFs) are responsible for these disease symptoms [1]. Substantial evidence suggests the involvement of insulin-like growth factor 1 receptor (IGF-1R) in GO [2]. TSHR and IGF-1R, which are OF surface receptors, stimulate hyaluronic acid synthesis and de novo adipogenesis through peroxisome proliferator-activated receptor gamma (PPAR-γ) [3, 4].

Based on the molecular pathogenesis of GO, medical and surgical treatments of patients with GO have been implemented. In particular, corticosteroids and orbital radiotherapy continue to be used to treat patients with GO [5]. Orbital radiotherapy combined with corticosteroids protects against disease

progression by reducing compressive optic neuropathy in patients with active thyroid eye disease [6]. However, glucocorticoid therapy has a negative effect on patient hyperthyroid status and adrenal insufficiency, as well as acute liver damage, when alanine aminotransferase levels are greater than 300 U/L [7, 8]. Moreover, medical radiotherapy also resulted in the development of malignancies, depending on the age and gender of patients [9].

Placenta-derived mesenchymal stem cells (PD-MSCs) have been broadly investigated due to their multilineage differentiation potential, and these cells have especially potent immunomodulatory abilities associated with tissue repair and regenerative medicine. MSCs inhibit the proliferation of T, B, natural killer, and dendritic cells. Due to these immunoregulatory properties, the safety and clinical efficacy of MSC-based therapy has been tested in preclinical transplantation studies [10]. In comparison to other MSCs, PD-MSCs have an additional immunomodulatory advantage by regulating the expression of human leukocyte antigen (HLA)-ABC and HLA-G [11]. Hence, the therapeutic effects of PD-MSCs are considered to be associated with immunosuppression-mediated replacement of damaged tissues.

Phosphatase of regenerating liver-1 (PRL-1), also known as protein tyrosine phosphatase type IVA member 1 (PTP4A1) and PTPCAAX1, is a member of a small class of prenylated PTPs. PRL-1 was originally identified as an immediate early gene during liver regeneration [12]. PRL-1 contains the C-terminal prenylation motif for farnesylation CAAX [13]. PRL-1 promotes cellular proliferation during protein prenylation, which is a posttranslational lipid modification, by upregulating RhoA via the mevalonate metabolic pathway. The major enzyme HMG-CoA reductase regulates AMPK during protein prenylation through PRL-1 [14]. Moreover, PRL-1 modulates the oxidative stress response in the mammalian retina [15]. PRL-2, which is in the same class and subfamily as PRL-1 and has a similar amino acid sequence, plays an important role in hematopoietic stem cell self-renewal.

Recently, we reported therapeutic effects of the application of naïve PD-MSCs in a GO mouse model [16]. However, it is still unknown whether functionally enhanced PD-MSCs overexpressing PRL-1 (PD-MSCs^{PRL-1}, PRL-1+) inhibit adipogenesis in OFs from GO patients to exert therapeutic effects.

Materials And Methods

Cell culture and gene transfection

Orbital adipose tissue specimens were obtained from patients with Graves' ophthalmopathy (GO) (n = 3) during fat decompression and from control individuals without a history of GO (n = 3) under consent conditions. Orbital fibroblasts (OFs) preparation was approved by the Institutional Review Board of CHA Bundang Medical Center, Seongnam, Republic of Korea (IRB-2018-01-007). Orbital tissue explants were minced and treated with 0.25 mg/mL collagenase (Sigma-Aldrich, St. Louis, MO, USA) for 1 h at 37 °C in a shaking incubator. After collagenase digestion, the orbital tissues were placed in culture plates with DMEM/F12 supplemented with 20% fetal bovine serum (FBS; Gibco, Carlsbad, CA, USA) and 1% penicillin/streptomycin (P/S; Gibco).

Placentas were collected for research purposes by the Institutional Review Board of CHA Gangnam Medical Center, Seoul, Republic of Korea (IRB 07-18). PD-MSCs were isolated as previously described [17] and cultured in α-modified minimal essential medium (α-MEM; HyClone Logan, UT, USA) supplemented with 10% FBS (Gibco), 1% P/S (Gibco), 1 μg/mL heparin (Sigma-Aldrich), and 25 ng/mL human fibroblast growth factor-4 (hFGF-4; Peprotech, Rocky Hill, NJ, USA). The PRL-1 plasmid vector was purchased from Origene (#RG200435; Rockville, MD, USA). To induce overexpression of the PRL-1 gene, naïve PD-MSCs (passage = 7) were transfected using the AMAXA nucleofector system (Lonza, Basel, Switzerland) according to the manufacturer's instructions. After transfection for 24 h, the cells were selected by 1.5 mg/mL neomycin. All cells were maintained at 37°C in a humidified atmosphere containing 5% CO_2.

Differentiation of PD-MSCs^{PRL-1} and OFs from GO patients

To analyze the potential of PD-MSCs^{PRL-1} to differentiate into mesodermal lineages, PD-MSCs^{PRL-1} (passage = 5) were plated at a density of 5×10^3 cells/cm^2 in various differentiation induction media using the StemPro adipogenesis and osteogenesis differentiation kit (Gibco) according to the manufacturer's instructions. After approximately 21 days, PD-MSCs^{PRL-1} were fixed in 4% paraformaldehyde and incubated for 1 h with Oil Red O (Sigma-Aldrich) to stain lipids to visualize lipid vesicles and von Kossa with 5% silver nitrate (Sigma-Aldrich) under the light to evaluate the accumulation of calcium deposits.

To induce adipogenic differentiation, normal and GO-derived OFs (5×10^3 cells/cm^2) were seeded and incubated in serum-free DMEM/F12 supplemented with 33 μM biotin, 17 μM pantothenic acid, 10 μg/mL transferrin, 0.2 nM triiodothyronine (T_3), 1 μM insulin (all from Sigma-Aldrich), 0.2 μM carbaprostacyclin ($cPGI_2$; Cayman Chemical, Ann Arbor, MI, USA), 1 μM dexamethasone, and 0.1 mM isobutylmethylxanthine (IBMX; all from Sigma-Aldrich) for the first 4 days. To induce the maturation of adipocytes, the medium was supplemented except 1 μM dexamethasone and 0.1 mM IBMX (all from Sigma-Aldrich) for 6 days and was replaced every other day. Lipid accumulation and adipocyte morphology were visualized by Oil Red O staining. The individual experiment was performed in triplicate.

Coculture experiments

To detect the inhibition of adipogenesis, normal and GO-derived OFs underwent adipogenic differentiation and were cocultured with naïve and PD-MSCs^{PRL-1} (5×10^3 cells/cm^2) in Transwell inserts (8 μm pore size; Corning, NY, USA) in α-MEM (HyClone) supplemented with 10% FBS and 1% P/S (all from Gibco) for 24 h at 37 °C in a humidified atmosphere containing 5% CO_2. The individual experiment was performed in triplicate.

Reverse transcription polymerase chain reaction (RT-PCR) and quantitative real-time PCR (qRT-PCR)

Total RNA was extracted using TRIzol LS reagent (Invitrogen, Carlsbad, CA, USA) according to the manufacturer's protocol. The concentration and purity of the total RNA were determined

spectrophotometrically by measuring the ODs at 260 nm and 280 nm. cDNA was reverse transcribed from total RNA (500 ng) by using SuperScript III reverse transcriptase (Invitrogen). To analyze stemness markers in PD-MSCs^{PRL-1}, PCR amplification was performed with specific primers (Table 1). β-actin was used as an internal control. The amplified PCR products were electrophoresed on 2% agarose gels containing 1.5 μg/mL ethidium bromide and visualized under UV light. qRT-PCR analysis was used to determine differences in gene expression. qRT-PCR was performed with primers (Table 2) and SYBR Green PCR master mix (Roche, Basel, Switzerland) in a CFX Connect™ Real-Time System (Bio-Rad, Hercules, CA, USA). All reactions were performed in triplicate.

Table 1
Primer sequences using reverse transcription polymerase chain reaction

Genes	Primer sequences	Tm
Oct4	Forward5'-AGTGAGAGGCAACCTGGAGA-3'	52
	Reverse 5'-GTGAAGTGAGGGCTCCCATA-3'	
Nanog	Forward5'-TTCTTGACTGGGACCTTGTC-3'	52
	Reverse 5'-GCTTGCCTTGCTTTGAAGCA-3'	
Sox2	Forward5'-GGGCAGCGTGTACTTATCCT-3'	52
	Reverse 5'-AGAACCCCAAGATGCACAAC-3'	
HLA-G	Forward5'-GCGGCTACTACAACCAGAGC-3'	58
	Reverse 5'-GCACATGGCACGTGTATCTC-3'	
TERT	Forward5'-GAGCTGACGTGGAAGATGAG-3'	55
	Reverse 5'-CTTCAAGTGCTGTCTGATTCCAATG-3'	
AFP	Forward5'-ATGCTGCAAACTGACCACGC-3'	55
	Reverse 5'-GCTTCGCTTTGCCAATGCTT-3'	
Albumin	Forward5'-TGAGTTTGCAGAAGTTTCCA-3'	60
	Reverse 5'-CCTTTGCCTCAGCATAGTTT-3'	
β-actin	Forward5'-TCCTTCTGCATCCTGTCAGCA-3'	58
	Reverse 5'-CAGGAGATGGCCACTGCCGCA-3'	

Table 2
Primer sequences using quantitative real time polymerase chain reaction

Genes	Primer sequences	Tm
OC	Forward5'-AGTGAGAGGCAACCTGGAGA-3'	52
	Reverse 5'-GTGAAGTGAGGGCTCCCATA-3'	
COL1A1	Forward5'-TTCTTGACTGGGACCTTGTC-3'	52
	Reverse 5'-GCTTGCCTTGCTTTGAAGCA-3'	
Adipsin	Forward5'-GGGCAGCGTGTACTTATCCT-3'	52
	Reverse 5'-AGAACCCCAAGATGCACAAC-3'	
PPAR-γ	Forward5'-GCGGCTACTACAACCAGAGC-3'	58
	Reverse 5'-GCACATGGCACGTGTATCTC-3'	
Adiponectin	Forward5'-GAGCTGACGTGGAAGATGAG-3'	55
	Reverse 5'-CTTCAAGTGCTGTCTGATTCCAATG-3'	
Leptin	Forward5'-ATGCTGCAAACTGACCACGC-3'	55
	Reverse 5'-GCTTCGCTTTGCCAATGCTT-3'	
LPL	Forward5'-TGAGTTTGCAGAAGTTTCCA-3'	60
	Reverse 5'-CCTTTGCCTCAGCATAGTTT-3'	
FABP4	Forward5'-GCATGGCCAAACCTAACATGA-3'	55
	Reverse 5'-CCTGGCCCAGTATGAAGGAAA-3'	
IGFBP1	Forward5'-GAGCCCTGCCGAATAGAAC-3'	60
	Reverse 5'-GGATCCTCTTCCCATTCCAAG-3'	
IGFBP2	Forward5'-ACATCCCCAACTGTGACAAG-3'	60
	Reverse 5'-ATCAGCTTCCCGGTGTTG-3'	
IGFBP3	Forward5'-CAGAGCACAGATACCCAGAAC-3'	60
	Reverse 5'-AGCACATTGAGGAACTTCAGG-3'	
IGFBP4	Forward5'-CTGACAGCTTTCGAGAGTGAG-3'	60
	Reverse 5'-GCGCATTTGAGGGAAACTTC-3'	
IGFBP5	Forward5'-ACCCAGTCCAAGTTTGTCG-3'	60
	Reverse 5'-TGTAGAATCCTTTGCGGTCAC-3'	
IGFBP6	Forward5'-GTCTACACCCCTAACTGCG-3'	60
	Reverse 5'-CTCTGTTGGTCTCTGCGG-3'	
IGFBP7	Forward5'-GCCCAGAAAAGCATGAAGTAAC-3'	60
	Reverse 5'-TTTATAGCTCGGCACCTTCAC-3'	
ITGA4	Forward5'-AGAGAGACAATCAGTGGTTGG-3'	55
	Reverse 5'-TCAGTTCTGTTCGTAAATCAGG-3'	
ITGB7	Forward5'-AGCAGCAACAACTCAACTGG-3'	55
	Reverse 5'-TTACAGACCCACCCTTCCTCT-3'	
FAK	Forward5'-GAAGCATTGGGTCGGGAACTA-3'	55
	Reverse 5'-CTCAATGCAGTTTGGAGGTGC-3'	
GAPDH	Forward5'-TCCTTCTGCATCCTGTCAGCA-3'	58
	Reverse 5'-CAGGAGATGGCCACTGCCGCA-3'	

Flow cytometry analysis

For immunophenotyping of cell surface antigens, third-passage PD-MSCs^{PRL-1} were detached, stained with antibodies conjugated with fluorescein isothiocyanate (FITC) and phycoerythrin (PE) and analyzed with a FACSCalibur flow cytometer (Becton Dickinson, Franklin Lakes, NJ, USA). The following monoclonal antibodies were used: CD34-PE, CD90-PE, HLA-ABC-FITC, HLA-DR-FITC (BD Bioscience, San

Jose, CA, USA), CD13-PE (BioLegend, San Diego, CA, USA), CD105-FITC (R&D Systems, Minneapolis, MN, USA), and HLA-G (Abcam, Cambridge, UK). For each sample, at least 10,000 events were acquired.

Teratoma formation and histological analysis

Nine-week-old male NOD/SCID mice (Laboratory Animal Research Center, Bungdang CHA Medical Center, CHA University, Seongnam, Republic of Korea) were maintained in an air-conditioned animal house under specific pathogen-free conditions. To investigate teratoma formation, PD-MSCs^{PRL-1} (5×10^5 cells) were directly injected into each testis (TP; $n = 2$). Control mice were not injected with cells (Con; $n = 2$). After 14 weeks, the testes were collected, and all mice were sacrificed. The testes were fixed in 10% neutral buffered formalin and embedded in paraffin. Sections were stained with hematoxylin and eosin (H&E).

Western blotting

Total protein was isolated lysis buffer (Sigma-Aldrich). The protein lysates were separated by 8 to 12% sodium dodecyl sulfate polyacrylamide gel electrophoresis (SDS-PAGE) and transferred to polyvinylidene difluoride (PVDF) membranes, which were then blocked in 5% bovine serum albumin and incubated overnight at 4 °C with the following primary antibodies: anti-PI3K p110α (1:1000, Cell Signaling Technology, Danvers, MA), anti-pAKT (1:1000, Cell Signaling Technology), anti-pmTOR (1,1000, Abcam), anti-phospho-focal adhesion kinase (pFAK; 1:1000, Cell Signaling Technology), anti-PPAR-γ (1:500, Santa Cruz Biotechnology, Dallas, TX), anti-leptin (1:500, R&D systems), anti-TNF-α (1:500, Santa Cruz Biotechnology), and anti-GAPDH (1:3000, AbFrontier, Seoul, Republic of Korea). The membranes were then incubated with horseradish peroxidase (HRP)-conjugated secondary antibodies (Bio-Rad, Hercules, CA, USA), and the bands were detected using an enhanced-chemiluminescence reagent (Bio-Rad). The individual experiment was performed in duplicate.

Statistical analysis

The experimental results are expressed as the means ± SD. Statistical analyses were performed using Student's t-tests and one way ANOVA and differences were considered statistically significant when the p value was less than 0.05. Each experiment was conducted in duplicate or triplicate.

Results

Characterization of PD-MSCs modified with the PRL-1 gene

PD-MSCs were transfected with the PRL-1 gene using a nonviral AMMXA system (Fig. 1a). After transfection, PRL-1 expression in PD-MSCs was verified by expression of the green fluorescent protein (GFP) reporter gene (Fig. 1b). The mRNA and protein expression levels of PRL-1 in PD-MSCs overexpressing PRL-1 (PD-MSCs^{PRL-1}, PRL-1+) were significantly higher than those in naïve cells (Fig. 1c, d). To confirm that PD-MSCs^{PRL-1} were similar to naïve cells, we measured the mRNA expression of genes associated with stemness markers, such as Oct4, Nanog and Sox2, telomerase reverse transcriptase

(TERT), and HLA-G. As expected, PD-MSCs^{PRL-1} were well maintained at passages 1 and 6 (Fig. 1e). To identify the phenotypes of PD-MSCs, the cell surface markers on PD-MSCs^{PRL-1} were analyzed by flow cytometry. PD-MSCs^{PRL-1} were positive for the expression of the MSC markers CD13, CD90, and CD105 but were negative for the hematopoietic lineage markers CD34 and HLA-DR; however, the HLA class I molecule HLA-ABC was highly expressed (Fig. 1f). Additionally, no teratoma formation was observed after transplantation of PD-MSCs^{PRL-1} (Fig. 1g).

To further evaluate the mesodermal lineage differentiation potential of PD-MSCs^{PRL-1}, the cells were exposed to osteogenic and adipogenic induction conditions. Successful osteogenic and adipogenic differentiation of PD-MSCs^{PRL-1} was evaluated by positive staining with von Kossa and Oil Red O, respectively (Fig. 1h). We previously confirmed the multidifferentiation potential of naïve MSCs [18]. After differentiation, osteogenic-specific markers (Osteocalcin; OC and Collagen Type 1 alpha 1; COL1A1) and adipogenic-specific markers (Adipsin and PPAR-γ) were expressed at high levels in differentiated PD-MSCs^{PRL-1}, as determined by qRT-PCR (Fig. 1i, j). These findings suggest that PD-MSCs^{PRL-1} maintain characteristics to those of naïve cells.

PD-MSCs^{PRL-1} inhibit adipogenesis in OFs from GO patients

To evaluate the effects of PD-MSCs^{PRL-1} on adipogenesis in OFs from GO patients, adipogenesis was induced in normal and GO-derived OFs for 4 days, followed by 6 days of maturation. After 10 days of in vitro maturation, differentiated GO-derived OFs were indirectly cocultured with naïve PD-MSCs and PD-MSCs^{PRL-1} (Fig. 2a). Normal and GO-derived OFs were induced to undergo adipogenesis and were stained using Oil Red O to visualize lipid accumulation (Fig. 2b). The mRNA expression levels of adipogenic-specific markers (adipsin, adiponectin, PPAR-γ, leptin, lipoprotein lipase; LPL, and fatty acid-binding protein 4; FABP4) in OFs from GO that were cocultured with naïve PD-MSCs and PD-MSCs^{PRL-1} were decreased compared to those of cells that were not cocultured. Interestingly, adiponectin, leptin, and LPL expression in cocultured PD-MSCs^{PRL-1} was significantly decreased compared with that of cocultured naïve PD-MSCs. Moreover, PPAR-γ, which is a transcription factor associated with de novo adipogenesis in OFs from GO patients, was downregulated in cells cocultured with PD-MSCs^{PRL-1} compared with cells cocultured with the naïve controls (Fig. 2c). These findings suggest that PD-MSCs^{PRL-1} downregulate the gene expression of adipogenic markers and inhibit adipogenesis in OFs from GO patients.

PD-MSCs^{PRL-1} promote the expression of IGFBP genes

IGFBPs control IGF-1R actions by regulating the bioavailability of the ligands IGF-1 and IGF-2 and have been shown to have inhibitory effects on adipogenesis in human visceral adipocytes. We previously analyzed whether naïve PD-MSCs and PD-MSCs^{PRL-1} secreted IGFBPs with a multiplex cytokine array (data not shown). Therefore, we investigated whether PD-MSCs^{PRL-1} promoted the expression of IGFBPs. qRT-PCR analysis revealed that the expression levels of IGFBP-2, -4, -6, and -7 in PD-MSCs^{PRL-1} were significantly elevated, although IGFBP-3 and -5 were reduced compared to those in naïve cells. These

data show that PD-MSCs^{PRL-1} upregulate the expression of IGFBP-2, -4, and -7 and may control IGFBP secretion (Fig. 3).

PD-MSC^{PRL-1}-induced IGFBPs inhibit adipogenesis via upregulation of FAK and downregulation of the PI3K/AKT/mTOR signaling pathway

We confirmed that the increased expression of adipogenic-specific genes in OFs from GO patients was downregulated by PD-MSCs^{PRL-1}. Moreover, the protein expression of PPAR-γ in OFs derived from GO patients cocultured with PD-MSCs^{PRL-1} was decreased compared to that of OFs that were cocultured with naïve PD-MSCs (Fig. 4a, b). Although there were no apparent differences in TNF-α expression between the naïve and cocultured groups (Fig. 4d), leptin expression in the PD-MSCs^{PRL-1} coculture group was markedly decreased compared with that in the naïve coculture group (Fig. 4c). To further investigate the mechanism by which PD-MSCs^{PRL-1} inhibit IGF-1-mediated adipogenesis signaling, we analyzed the expression levels of PI3K/AKT/mTOR pathway members by western blot analysis. The protein expression of phosphorylated PI3K, AKT, and mTOR in OFs from GO patients cocultured with PD-MSCs^{PRL-1} was significantly downregulated compared to that of cells that were not cocultured. Interestingly, PD-MSC^{PRL-1} coculture with OFs also decreased the levels of phosphorylated PI3K and the expression of downstream AKT and mTOR compared with those of the naïve coculture group (Fig. 4e).

In general, integrins are transmembrane receptors that facilitate cell-extracellular matrix adhesion and can interact with IGFBPs. To confirm that the PD-MSC^{PRL-1}-mediated increase in IGFBPs in OFs from GO patients contributes to regulating the adipogenic effect through the integrin signaling pathway, we investigated the expression of ITGA4 and ITGB7 and the integrin downstream signaling factor FAK in normal and GO-derived OFs cocultured with PD-MSCs^{PRL-1}. The mRNA expression levels of ITGA4 and ITGB7 in normal and GO-derived OFs cocultured with PD-MSCs^{PRL-1} were higher than those in noncocultured OFs (Fig. 4f, g). Moreover, the mRNA expression of FAK, which is a downstream factor of ITGA4 and ITGB7, in normal and GO-derived OFs cocultured with PD-MSCs^{PRL-1} was significantly higher than that in OFs cocultured with naïve PD-MSCs (Fig. 4 h). As shown in Fig. 4e, the mRNA level of FAK was consistent with the protein level. These findings suggest that enhanced IGFBP expression by PD-MSCs^{PRL-1} promotes ITGA4 and ITGB7 signaling, which leads to FAK activation and downregulates the PI3K/AKT/mTOR signaling pathway, resulting in inhibition of OF adipogenesis (Fig. 5).

Discussion

MSCs have immunomodulatory roles in autoimmune diseases, including GO [19]. Because medical therapies, including corticosteroids and radiotherapy, for patients with GO lead to side effects and the development of malignancies, understanding the molecular mechanisms of de novo adipogenesis and the main symptoms of GO is critical in developing therapeutic applications. In particular, MSCs have immunosuppressive effects on antigen presenting cells and secrete soluble factors, including adipokines [20]. Previous reports showed that PD-MSCs have more immunological advantages than other MSCs, as

evidenced by the increased expression of HLA-G and the cytokines of IL-2, IL-4, IL-13, and GM-CSF [11]. However, MSC aging results in limited self-renewal abilities and age-associated decreases in cellular numbers and functions [21]. Therefore, gene modification using gene delivery systems overcomes the limited functions of MSCs to provide effective therapeutic results [22]. A recent report revealed that genetically modified MSCs overexpressing IL-35 could be applied in autoimmune diseases to overcome the complications of long-term immunosuppression [23]. In our previous study, we generated TERT-overexpressing PD-MSCs using a nonviral AMAXA system to study the underlying regulatory mechanisms of self-renewal [24].

PRL-1 is a member of a subgroup of related protein tyrosine phosphatases contacting a C-terminal prenylation motif [13]. C-terminal residues and cellular redox environments are controlled by the enzymatic activity of PRL-1 [25]. In oxidative-stressed retinas and photoreceptors, modulation of PRL-1 activity regulates redox conditions [15]. We hypothesized that PD-MSCs^{PRL-1} would regulate oxidative conditions and reduce adipogenesis in OFs from GO patients. Because little is known about the efficacy of PD-MSC^{PRL-1}-mediated inhibition of adipogenesis in OFs from GO patients, we further analyzed the functional enhancement of PRL-1 in PD-MSCs generated using a nonviral AMAXA system. OFs isolated from patients with GO are capable of adipocyte differentiation [3]. In orbital adipose tissues and in vitro GO-derived OFs after differentiation, enhanced adiponectin, leptin and PPAR-γ were positively correlated [26]. Previous reports demonstrated that IGF-1 expression was enhanced and PI3K was activated by upregulating PPAR-γ in the orbital fatty connective tissue of patients with GO [27].

In general, IGF binds to IGFBPs. Individual IGFBPs act to increase or attenuate the IGF signaling pathway [28]. IGFBP2 prevents adipogenesis [29], and IGFBP3 interferes with PPAR-γ-dependent processes to impair adipocyte differentiation [30]. Overexpressed IGFBP2 inhibits both lipogenesis and adipogenesis in visceral adipocytes, and this process involves cell surface-associated IGFBP2 activating the integrin signaling pathway [31]. Similarly, IGFBP4 controls the expression of insulin and IGF1 in mouse adipose tissue expansion [32]. Because we previously analyzed whether naïve PD-MSCs and PD-MSCs^{PRL-1} significantly secreted IGFBPs using a multiplex cytokine array (data not shown), we found that PD-MSCs^{PRL-1} secreted IGFBP2, -4, and -7 and inhibited adipogenesis. ITGA4- and ITGB7-mediated enhanced secretion of IGFBPs by PD-MSCs^{PRL-1} decreased PPAR-γ-dependent processes via downregulation of PI3K/AKT/mTOR activities and inhibited adipogenesis.

Conclusions

In this study, we showed that PD-MSCs modified with the PRL-1 gene using nonviral transfection method efficiently overexpressed the PRL-1 protein and maintained the phenotype and multilineage differentiation properties of MSCs. PD-MSCs^{PRL-1} induced IGFBP expression and inhibited adipogenesis via upregulation of FAK and downregulation of the PI3K/AKT/mTOR signaling pathway in OFs from GO patients. In this study, we focused on overcoming the medical problems of GO patients, and functional

enhancement of PD-MSCs by nonviral gene modification provides novel insight into next-generation MSC-based cell therapy for future clinical trials in immunological diseases.

Abbreviations

COL1A1: Collagen type 1 alpha 1; FABP4: Fatty acid-binding protein 4; FAK: Focal adhesion kinase; GFP: Green fluorescent protein; GO: Graves' ophthalmopathy; GVHD: Graft-versus-host-disease; IGF-1R: Insulin-like growth factor 1 receptor; ITGA4: Integrin alpha 4; LPL: Lipoprotein lipase; OC: Osteocalcin; OF: Orbital fibroblast; PD-MSCs: Placenta-derived mesenchymal stem cells; PPAR-γ: Peroxisome proliferator-activated receptor-gamma; PRL-1: Phosphatase of regenerating liver-1; TERT: Telomerase reverse transcriptase

Declarations

Acknowledgements

Not applicable.

Availability of data and materials

All data and materials are available upon request.

Author details

[1]Department of Biomedical Science, CHA University, Seongnam 13488, Republic of Korea; [2]Center for Non-Clinical Development, CHA Advanced Research Institute CHA University, Seongnam 13488, Republic of Korea; [3]Department of Ophthalmology, CHA Bundang Medical Center CHA University, Seongnam 13496, Republic of Korea

Author's contributions

JYK contributed to the analysis and interpretation of data and manuscript writing. H-JL did the data analysis. HL provided OF samples. SP and GJK reviewed the manuscript. GJK did financial support, and final approval of manuscript. All authors read and approved the final manuscript.

Ethics approval and consent to participate

The process of obtaining orbital adipose tissues was approved by the Institutional Review Board of Bundang CHA Medical Center (Seongnam, Republic of Korea, IRB-2018-01-007), and placenta tissues were collected for research purposes by the Institutional Review Board of CHA Gangnam Medical Center (Seoul, Republic of Korea, IRB 07-18). All patients consented to the proper use for research.

Consent for publication

Not applicable

Competing interests

The authors declare that they have no competing interests.

Funding

This research was supported by grants of the Korea Health Technology R&D Project through the Korea Health Industry Development Institute (KHIDI), funded by the Ministry of Health & Welfare, Republic of Korea (grant number : HI16C1599) and by Basic Science Research Program through the National Research Foundation of Korea (NRF) funded by the Ministry of Education (grant number: 2019R1I1A1A01057255).

References

1. Bahn RS. Graves' ophthalmopathy. N Engl J Med. 2010;362(8):726-38.
2. Mohyi M, Smith TJ. IGF1 receptor and thyroid-associated ophthalmopathy. J Mol Endocrinol. 2018;61(1):T29-T43.
3. Mimura LY, Villares SM, Monteiro ML, Guazzelli IC, Bloise W. Peroxisome proliferator-activated receptor-gamma gene expression in orbital adipose/connective tissues is increased during the active stage of Graves' ophthalmopathy. Thyroid. 2003;13(9):845-50.
4. Li B, Smith TJ. PI3K/AKT pathway mediates induction of IL-1RA by TSH in fibrocytes: modulation by PTEN. J Clin Endocrinol Metab. 2014;99(9):3363-72.
5. Ponto KA, Zang S, Kahaly GJ. The tale of radioiodine and Graves' orbitopathy. Thyroid. 2010;20(7):785-93.
6. Shams PN, Ma R, Pickles T, Rootman J, Dolman PJ. Reduced risk of compressive optic neuropathy using orbital radiotherapy in patients with active thyroid eye disease. Am J Ophthalmol. 2014;157(6):1299-305.
7. Giotaki Z, Fountas A, Tsirouki T, Bargiota A, Tigas S, Tsatsoulis A. Adrenal reserve following treatment of Graves' orbitopathy with intravenous glucocorticoids. Thyroid. 2015;25(4):462-3.
8. Moleti M, Giuffrida G, Sturniolo G, Squadrito G, Campenni A, Morelli S et al. Acute liver damage following intravenous glucocorticoid treatment for Graves' ophthalmopathy. Endocrine. 2016;54(1):259-68.
9. Mazonakis M, Tzedakis A, Lyraraki E, Damilakis J. Risk of developing radiogenic cancer following photon-beam radiotherapy for Graves' orbitopathy. Med Phys. 2018;45(10):4775-82.
10. Diehl R, Ferrara F, Muller C, Dreyer AY, McLeod DD, Fricke S, Boltze J. Immunosuppression for in vivo research: state-of-the-art protocols and experimental approaches. Cell Mol Immunol. 2017;14(2):146-79.

11. Lee JM, Jung J, Lee HJ, Jeong SJ, Cho KJ, Hwang SG, Kim GJ. Comparison of immunomodulatory effects of placenta mesenchymal stem cells with bone marrow and adipose mesenchymal stem cells. Int Immunopharmacol. 2012;13(2):219-24.
12. Rios P, Li X, Kohn M. Molecular mechanisms of the PRL phosphatases. FEBS J. 2013;280(2):505-24.
13. Si X, Zeng Q, Ng CH, Hong W, Pallen CJ. Interaction of farnesylated PRL-2, a protein-tyrosine phosphatase, with the beta-subunit of geranylgeranyltransferase II. J Biol Chem. 2001;276(35):32875-82.
14. Gao J, Liao J, Yang GY. CAAX-box protein, prenylation process and carcinogenesis. Am J Transl Res. 2009;1(3):312-25.
15. Yu L, Kelly U, Ebright JN, Malek G, Saloupis P, Rickman DW, McKay BS, Arshavsky VY, Bowes Rickman C. Oxidative stress-induced expression and modulation of Phosphatase of Regenerating Liver-1 (PRL-1) in mammalian retina. Biochim Biophys Acta. 2007;1773(9):1473-82.
16. Park M, Banga JP, Kim GJ, Kim M, Lew H. Human placenta-derived mesenchymal stem cells ameliorate orbital adipogenesis in female mice models of Graves' ophthalmopathy. Stem Cell Res Ther. 2019;10(1):246.
17. Lee MJ, Jung J, Na KH, Moon JS, Lee HJ, Kim JH et al. Anti-fibrotic effect of chorionic plate-derived mesenchymal stem cells isolated from human placenta in a rat model of CCl(4)-injured liver: potential application to the treatment of hepatic diseases. J Cell Biochem. 2010;111(6):1453-63.
18. Seok J, Jung HS, Park S, Lee JO, Kim CJ, Kim GJ. Alteration of fatty acid oxidation by increased CPT1A on replicative senescence of placenta-derived mesenchymal stem cells. Stem Cell Res Ther. 2020;11(1):1.
19. De Miguel MP, Fuentes-Julian S, Blazquez-Martinez A, Pascual CY, Aller MA, Arias J, Arnalich-Montiel F. Immunosuppressive properties of mesenchymal stem cells: advances and applications. Curr Mol Med. 2012;12(5):574-91.
20. Gentile P, Garcovich S. Concise Review: Adipose-Derived Stem Cells (ASCs) and Adipocyte-Secreted Exosomal microRNA (A-SE-miR) Modulate Cancer Growth and proMote Wound Repair. J Clin Med. 2019;8(6).
21. Li Y, Wu Q, Wang Y, Li L, Bu H, Bao J. Senescence of mesenchymal stem cells (Review). Int J Mol Med. 2017;39(4):775-82.
22. Nowakowski A, Walczak P, Lukomska B, Janowski M. Genetic Engineering of Mesenchymal Stem Cells to Induce Their Migration and Survival. Stem Cells Int. 2016;2016:4956063.
23. Guo H, Li B, Wang W, Zhao N, Gao H. Mesenchymal stem cells overexpressing IL-35: a novel immunosuppressive strategy and therapeutic target for inducing transplant tolerance. Stem Cell Res Ther. 2018;9(1):254.
24. Lee HJ, Choi JH, Jung J, Kim JK, Lee SS, Kim GJ. Changes in PTTG1 by human TERT gene expression modulate the self-renewal of placenta-derived mesenchymal stem cells. Cell Tissue Res. 2014;357(1):145-57.

25. Skinner AL, Vartia AA, Williams TD, Laurence JS. Enzyme activity of phosphatase of regenerating liver is controlled by the redox environment and its C-terminal residues. Biochemistry. 2009;48(20):4262-72.
26. Kumar S, Leontovich A, Coenen MJ, Bahn RS. Gene expression profiling of orbital adipose tissue from patients with Graves' ophthalmopathy: a potential role for secreted frizzled-related protein-1 in orbital adipogenesis. J Clin Endocrinol Metab. 2005;90(8):4730-5.
27. Zhao P, Deng Y, Gu P, Wang Y, Zhou H, Hu Y, Chen P, Fan X. Insulin-like growth factor 1 promotes the proliferation and adipogenesis of orbital adipose-derived stromal cells in thyroid-associated ophthalmopathy. Exp Eye Res. 2013;107:65-73.
28. Hwa V, Oh Y, Rosenfeld RG. The insulin-like growth factor-binding protein (IGFBP) superfamily. Endocr Rev. 1999;20(6):761-87.
29. Wheatcroft SB, Kearney MT, Shah AM, Ezzat VA, Miell JR, Modo M et al. IGF-binding protein-2 protects against the development of obesity and insulin resistance. Diabetes. 2007;56(2):285-94.
30. Chan SS, Schedlich LJ, Twigg SM, Baxter RC. Inhibition of adipocyte differentiation by insulin-like growth factor-binding protein-3. Am J Physiol Endocrinol Metab. 2009;296(4):E654-63.
31. Yau SW, Russo VC, Clarke IJ, Dunshea FR, Werther GA, Sabin MA. IGFBP-2 inhibits adipogenesis and lipogenesis in human visceral, but not subcutaneous, adipocytes. Int J Obes (Lond). 2015;39(5):770-81.
32. Gealekman O, Gurav K, Chouinard M, Straubhaar J, Thompson M, Malkani S, Hartigan C, Corvera S. Control of adipose tissue expandability in response to high fat diet by the insulin-like growth factor-binding protein-4. J Biol Chem. 2014;289(26):18327-38.

Figures

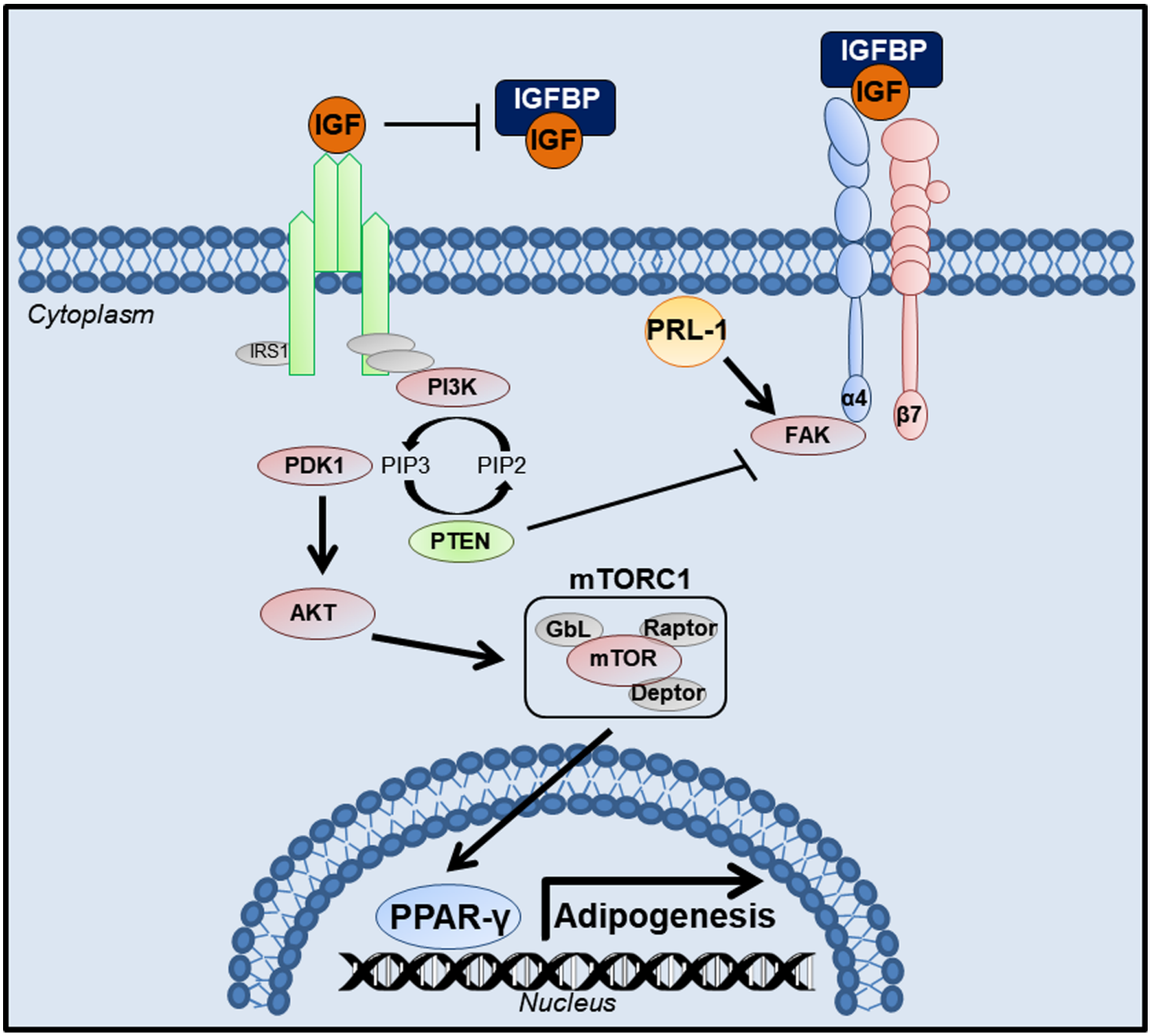

Figure 1

Summarized diagram proposes that anti-adipogenic key factor of secreted IGFBPs in PD-MSCsPRL-1 inhibit adipogenesis in OFs with GO patients through upregulation of FAK and downregulation of PI3K/AKT/mTOR signaling pathway.

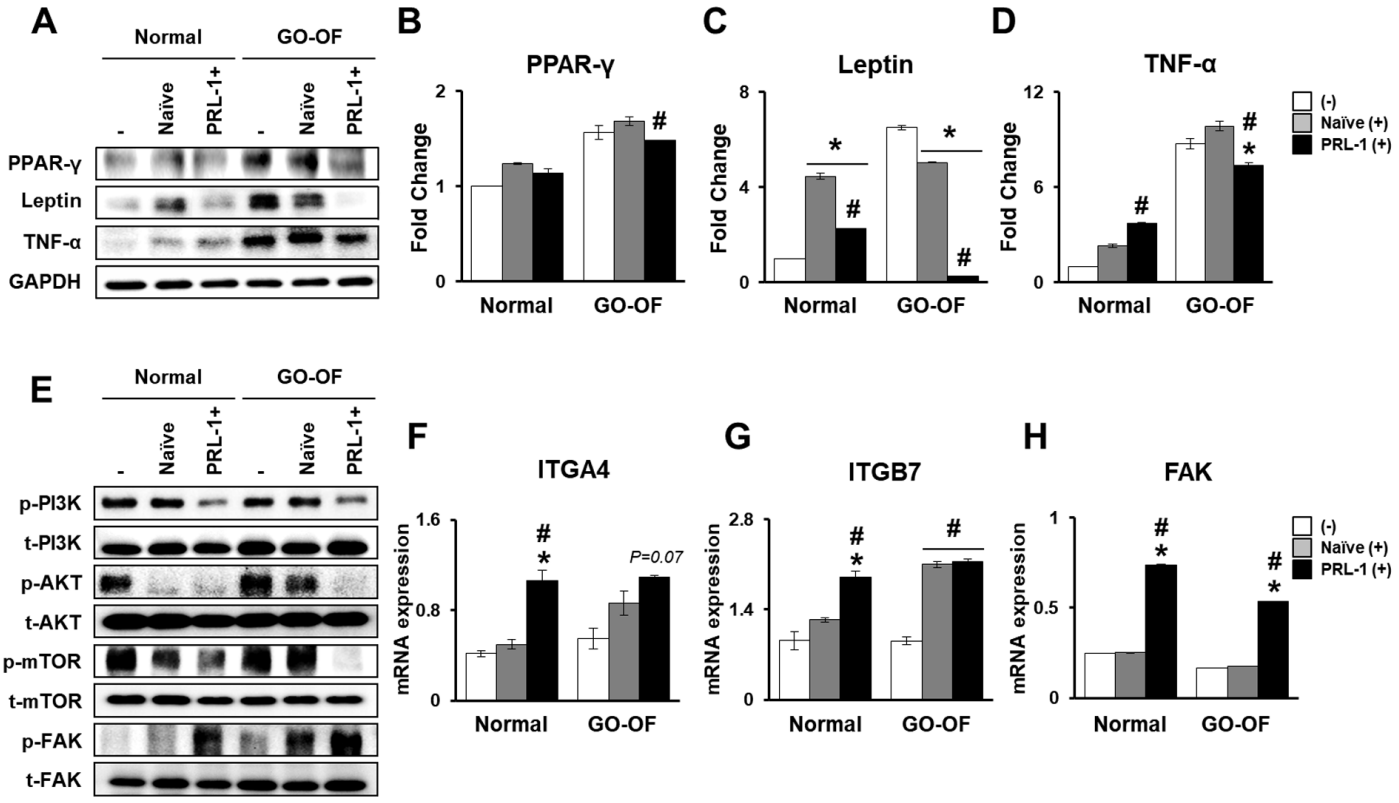

Figure 2

IGFBPs induced by PD-MSCsPRL-1 inhibit adipogenesis via upregulation of FAK and downregulation of PI3K/AKT/mTOR signaling pathway. a Protein expressions of PPAR-γ, Leptin, and TNF-α in normal and GO-derived OFs with naïve and PD-MSCsPRL-1 cocultivation after 24 h using western blotting. Quantitative analysis of b PPAR-γ c Leptin and d TNF-α in normal and GO-derived OFs with naïve and PD-MSCsPRL-1 cocultivation after 24 h (mean ± SD *p < 0.05 compared with non-cocultivation groups) (mean ± SD #p < 0.05 compared with naïve cocultivation groups). e Protein expressions of phospho/total-PI3K, AKT, mTOR, and FAK in normal and GO-derived OFs with naïve and PD-MSCsPRL-1 cocultivation after 24 h using western blotting. mRNA expression of f ITGA4, g ITGB7, and h FAK in normal and GO-derived OFs with naïve and PD-MSCsPRL-1 cocultivation after 24 h (mean ± SD *p < 0.05 compared with non-cocultivation groups) (mean ± SD #p < 0.05 compared with naïve cocultivation groups).

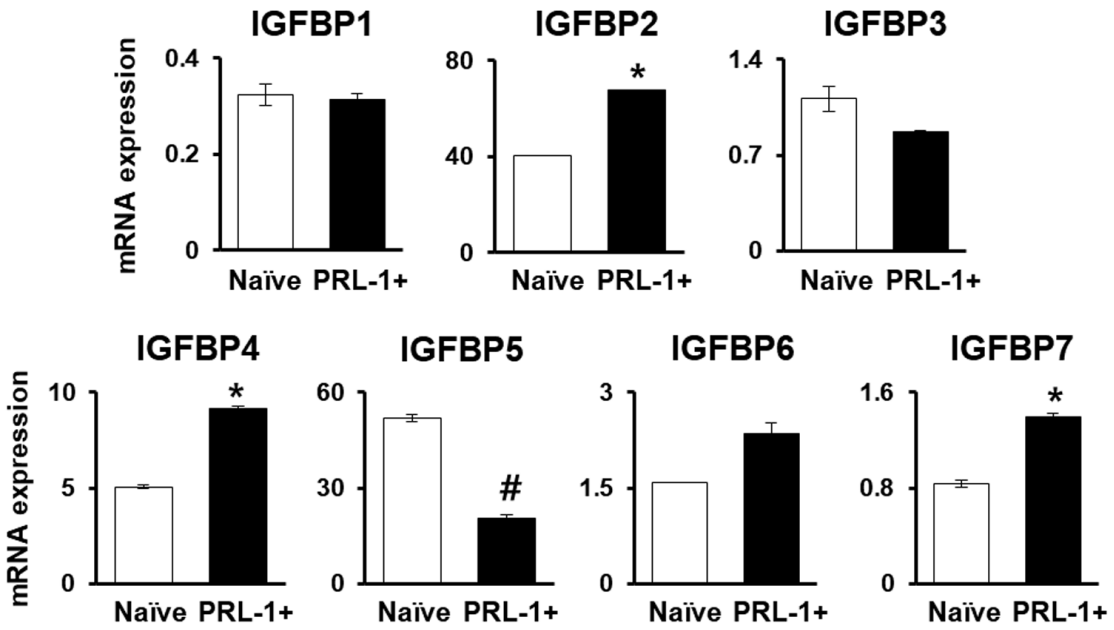

Figure 3

PD-MSCsPRL-1 promote expression of IGFBP genes. mRNA expression of IGFBPs in naïve and PD-MSCsPRL-1 using qRT-PCRs (mean ± SD *p < 0.05 compared with naïve) (mean ± SD #p < 0.05 compared with naïve).

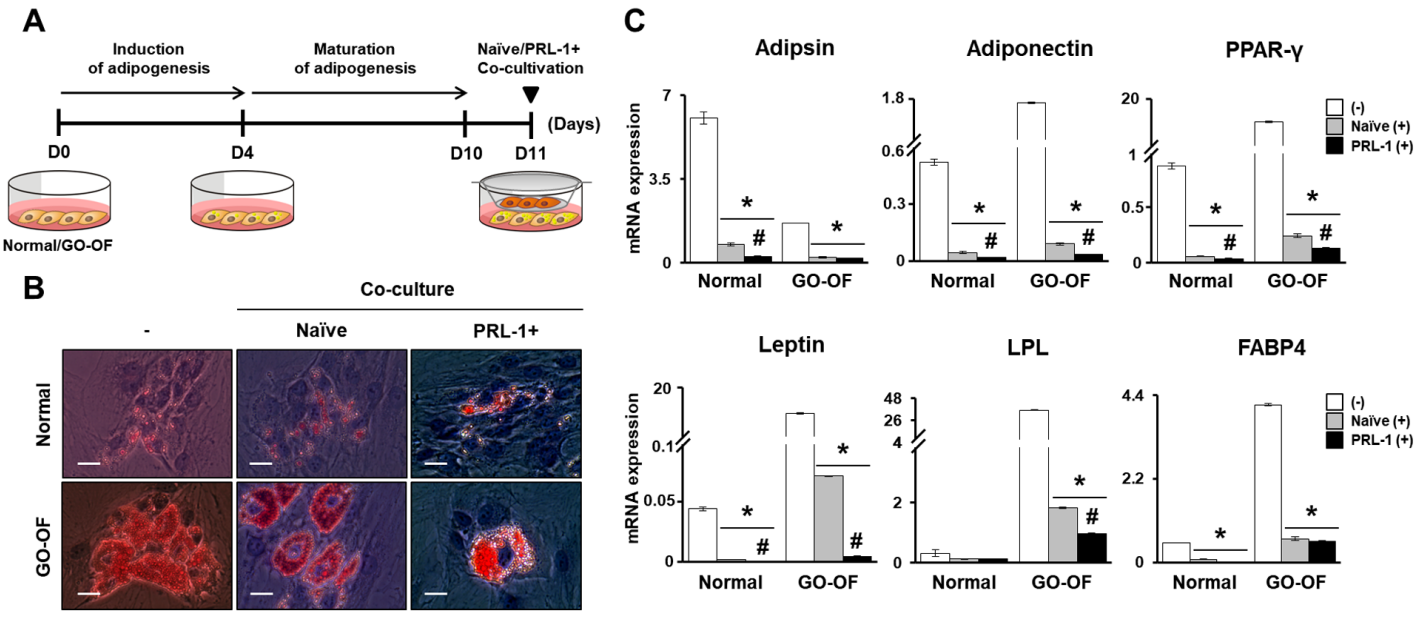

Figure 4

PD-MSCsPRL-1 inhibit adipogenesis OF with GO patients. a A schematic diagram describing the naïve and PD-MSCsPRL-1 cocultivation with adipogenesis differentiation in normal (n = 3) and OF with GO

patients (n = 3). During the first 4 days, adipogenesis in normal and GO-derived OFs was induced. From 10 days, normal and GO-derived OFs were maintained for maturation of adipogenesis. For 24 h, naïve and PD-MSCsPRL-1 in transwell insert system were cocultured. b Representative images of adipogenic differentiation in normal and GO-derived OFs with naïve and PD-MSCsPRL-1 cocultivation. Scale bars: 100 μm. c qRT-PCR analysis of mRNA adipogenic specific markers in normal and GO-derived OFs induced adipogenic differentiation according to naïve and PD-MSCsPRL-1 cocultivation. (mean ± SD *p < 0.05 compared with non cocultivation groups) (mean ± SD #p < 0.05 compared with naïve cocultivation groups).

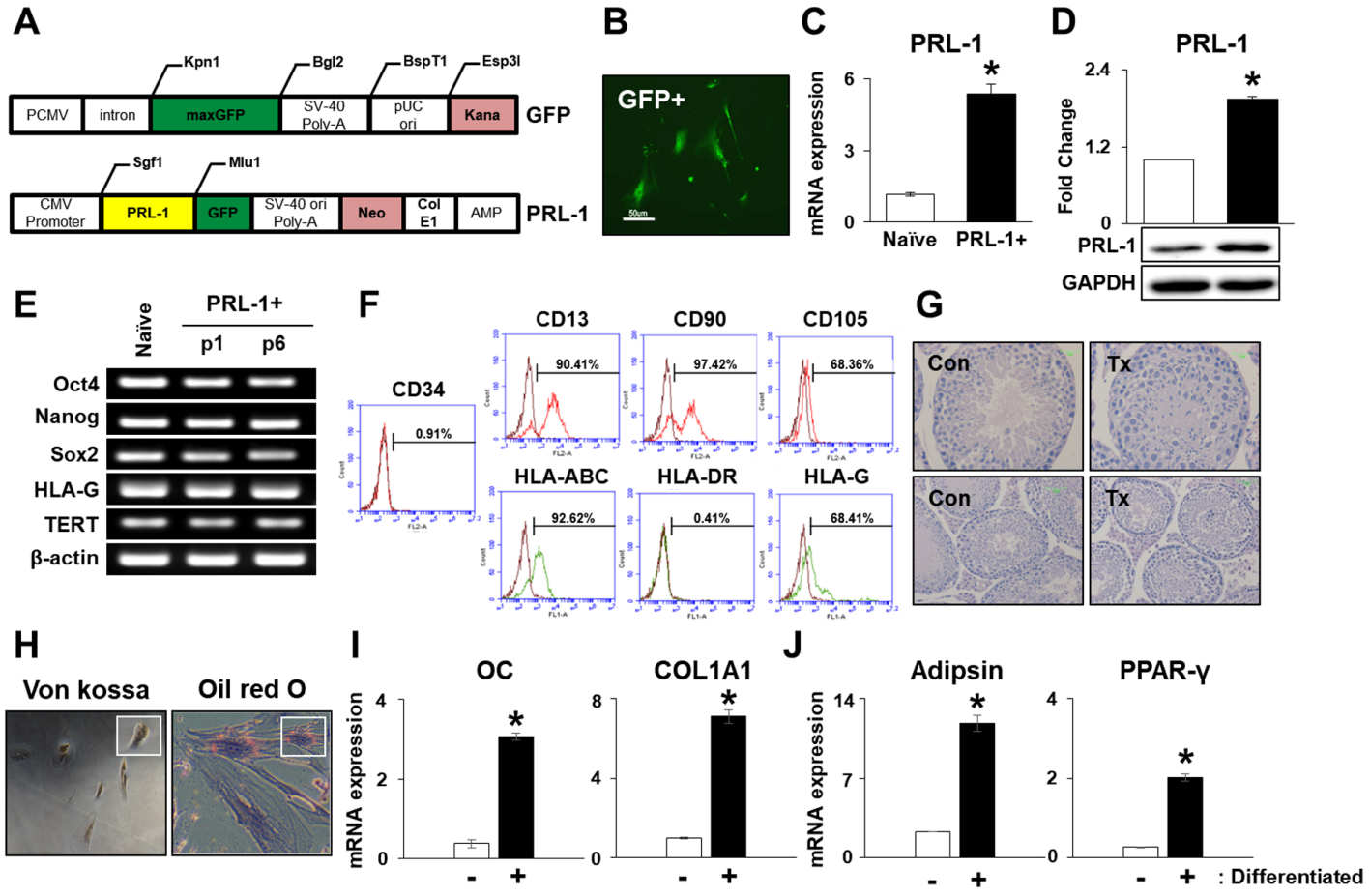

Figure 5

Characterization of PD-MSCs modified with PRL-1 gene. a GFP and PRL-1 plasmid vector map. b Expression of GFP in PD-MSCsPRL-1 using non-viral gene delivery system. Scale bars: 100 μm. c mRNA and d protein expressions of PRL-1 in PD-MSCsPRL-1 (mean ± SD *p < 0.05 compared with naïve). e Stemness markers in naïve and PD-MSCsPRL-1 depending on passages by RT-PCR. f Surface markers of hematopoietic, non-hematopoietic, and HLA family in PD-MSCsPRL-1 by FACS analysis. g Histopathological analysis of NOD/SCID mice testis and PD-MSCsPRL-1 transplanted in NOD/SCID mice testis after 14 weeks by H&E. h Osteogenic and adipogenic differentiations of PD-MSCsPRL-1 using von Kossa and Oil Red O staining. mRNA expression of i osteogenic- (OC and COL1A1) and j adipogenic-

specific markers in differentiated PD-MSCsPRL-1 (mean ± SD *p < 0.05 compared with undifferentiated groups).